Modeling compressible flows with Lattice-Boltzmann Methods

January 19, 2022

Gabriel Farag

Sous la supervision de Pierre Boivin et Guillaume Chiavassa

Faculté des Sciences
Aix-Marseille Université

M2P2

labex MEC
Mécanique Et Complexité

Table of contents

Lattice-Boltzmann basics

Moments, distributions, lattices, discretization

Navier-Stokes-Fourier system

Mass, momentum and energy conservations,

$$\frac{\partial \rho}{\partial t} + \frac{\partial \rho u_\beta}{\partial x_\beta} = 0\,, \tag{1}$$

$$\frac{\partial \rho u_\alpha}{\partial t} + \frac{\partial \left[\rho u_\alpha u_\beta + p\delta_{\alpha\beta} - T_{\alpha\beta}\right]}{\partial x_\beta} = 0\,. \tag{2}$$

$$\frac{\partial \rho(e + u_\alpha^2/2)}{\partial t} + \frac{\partial \left[(\rho(e + u_\alpha^2/2) + p)u_\beta + q_\beta - u_\alpha T_{\alpha\beta}\right]}{\partial x_\beta} = 0\,. \tag{3}$$

Equations of state, *e.g.*

$$p = \rho R T\,, \tag{4}$$

$$e = C_v T + e_0\,. \tag{5}$$

Constitutive equations,

$$q_\alpha = -\lambda \frac{\partial T}{\partial x_\alpha}\,, \tag{6}$$

$$T_{\alpha\beta} = \mu\left[\frac{\partial u_\alpha}{\partial x_\beta} + \frac{\partial u_\beta}{\partial x_\alpha} - \delta_{\alpha\beta}\frac{2}{3}\frac{\partial u_\gamma}{\partial x_\gamma}\right]. \tag{7}$$

Navier-Stokes-Fourier system

Mass, momentum and energy conservations,

$$\frac{\partial \rho}{\partial t} + \frac{\partial \rho u_\beta}{\partial x_\beta} = 0\,, \tag{1}$$

$$\frac{\partial \rho u_\alpha}{\partial t} + \frac{\partial \left[\rho u_\alpha u_\beta + p\delta_{\alpha\beta} - \mathcal{T}_{\alpha\beta}\right]}{\partial x_\beta} = 0\,. \tag{2}$$

$$\frac{\partial \rho(e + u_\alpha^2/2)}{\partial t} + \frac{\partial \left[(\rho(e + u_\alpha^2/2) + p)u_\beta + q_\beta - u_\alpha \mathcal{T}_{\alpha\beta}\right]}{\partial x_\beta} = 0\,. \tag{3}$$

Equations of state, *e.g.*

$$p = \rho R T\,, \tag{4}$$

$$e = C_v T + e_0\,. \tag{5}$$

Constitutive equations,

$$q_\alpha = -\lambda \frac{\partial T}{\partial x_\alpha}\,, \tag{6}$$

$$\mathcal{T}_{\alpha\beta} = \mu \left[\frac{\partial u_\alpha}{\partial x_\beta} + \frac{\partial u_\beta}{\partial x_\alpha} - \delta_{\alpha\beta}\frac{2}{3}\frac{\partial u_\gamma}{\partial x_\gamma}\right]\,. \tag{7}$$

Navier-Stokes-Fourier system

Mass, momentum and energy conservations,

$$\frac{\partial \rho}{\partial t} + \frac{\partial \rho u_\beta}{\partial x_\beta} = 0\,, \tag{1}$$

$$\frac{\partial \rho u_\alpha}{\partial t} + \frac{\partial \left[\rho u_\alpha u_\beta + p\delta_{\alpha\beta} - \mathcal{T}_{\alpha\beta}\right]}{\partial x_\beta} = 0\,. \tag{2}$$

$$\frac{\partial \rho(e + u_\alpha^2/2)}{\partial t} + \frac{\partial \left[(\rho(e + u_\alpha^2/2) + p)u_\beta + q_\beta - u_\alpha \mathcal{T}_{\alpha\beta}\right]}{\partial x_\beta} = 0\,. \tag{3}$$

Equations of state, *e.g.*

$$p = \rho R T\,, \tag{4}$$

$$e = C_v T + e_0\,. \tag{5}$$

Constitutive equations,

$$q_\alpha = -\lambda \frac{\partial T}{\partial x_\alpha}\,, \tag{6}$$

$$\mathcal{T}_{\alpha\beta} = \mu \left[\frac{\partial u_\alpha}{\partial x_\beta} + \frac{\partial u_\beta}{\partial x_\alpha} - \delta_{\alpha\beta}\frac{2}{3}\frac{\partial u_\gamma}{\partial x_\gamma}\right]\,. \tag{7}$$

Late 1980s, birth of Lattice-Boltzmann Methods

VOLUME 61, NUMBER 20 PHYSICAL REVIEW LETTERS 14 NOVEMBER 1988

Use of the Boltzmann Equation to Simulate Lattice-Gas Automata

Guy R. McNamara and Gianluigi Zanetti[(a)]

The Research Institutes, The University of Chicago, 5640 South Ellis Avenue, Chicago, Illinois 60637

Figure 1: Guy R. McNamara and Gianluigi Zanetti, first Lattice-Boltzmann Model.

LBM algorithm is basically :

- Collision, local step
- Streaming, memory-shift

➔ Attractive method ! ➔

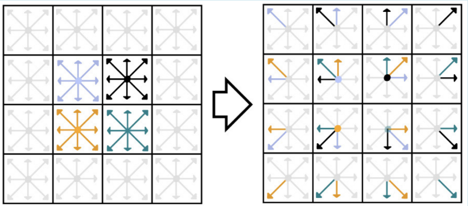

Figure 2: O'Brien's schematic streaming.

McNamara, G. R., & Zanetti, G. *Use of the Boltzmann equation to simulate lattice-gas automata*, Physical review letters, 1988.

O'Brien, P. M. *A framework for digital watercolor*, MSc thesis, Texas A&M University, 2008.

Velocity space discretization

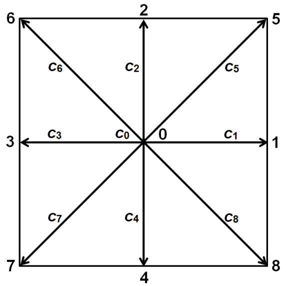

Figure 3: D2Q9 lattice.

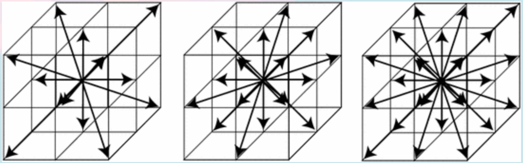

Figure 4: D3Q15, D3Q19 and D3Q27 lattices.

Each different lattice leads to a different Discrete Velocity Boltzmann Equation,

$$\frac{\partial f_i}{\partial t} + c_{i\alpha} \frac{\partial f_i}{\partial x_\alpha} = -\frac{1}{\tau}\left(f_i - f_i^{eq}\right) = -\frac{1}{\tau} f_i^{neq}\,, \tag{8}$$

$\boldsymbol{c}_i$ with $i = 0, \ldots, q\text{-}1$ and $f_i(t, \boldsymbol{x}) = f(t, x, \boldsymbol{c}_i)$.

- Discrete Velocity Boltzmann Equation (**DVBE**) with BGK collision kernel,

$$\frac{\partial f_i}{\partial t} + c_{i\alpha}\frac{\partial f_i}{\partial x_\alpha} = -\frac{1}{\tau}\left(f_i - f_i^{eq}\right) = -\frac{1}{\tau} f_i^{neq} . \tag{9}$$

- Integration along characteristic $d\boldsymbol{x} = \boldsymbol{c}_i dt$ and **Crank-Nicolson**,

$$f_i(t+\Delta t, \boldsymbol{x}+\boldsymbol{c}_i\Delta t) = f_i(t,\boldsymbol{x}) - \frac{\Delta t}{2}\left\{ \left[\frac{1}{\tau} f_i^{neq}\right](t,\boldsymbol{x}) + \left[\frac{1}{\tau} f_i^{neq}\right](t+\Delta t, \boldsymbol{x}+\boldsymbol{c}_i\Delta t)\right\} .$$

- Change of variables $\overline{f}_i = f_i + \frac{\Delta t}{2\tau} f_i^{neq}$ and $\overline{\tau} = \tau + \Delta t/2$,

$$\overline{f}_i(t+\Delta t, \boldsymbol{x}+\boldsymbol{c}_i\Delta t) = \left\{ f_i - \frac{\Delta t}{2\tau} f_i^{neq} \right\}(t,\boldsymbol{x}) , \tag{10}$$

$$= \left\{ f_i^{eq} + \left[1 - \frac{\Delta t}{2\tau}\right] f_i^{neq} \right\}(t,\boldsymbol{x}) , \tag{11}$$

$$= \left\{ f_i^{eq} + \left[1 - \frac{\Delta t}{\tau + \Delta t/2}\right] \overline{f}_i^{neq} \right\}(t,\boldsymbol{x}) . \tag{12}$$

By definition in Lattice-Boltzmann $f_i = f_i^{eq} + f_i^{neq}$:

$$\rho = \Pi^{f,(0)} = \sum_i f_i = \sum_i f_i^{eq}, \quad \rho u_\alpha = \Pi_\alpha^{f,(1)} = \sum_i c_{i\alpha} f_i = \sum_i c_{i\alpha} f_i^{eq}, \tag{13}$$

additionally, f_i^{eq} is also built such that,

$$\rho u_\alpha u_\beta + p\delta_{\alpha\beta} = \Pi_{\alpha\beta}^{f^{eq},(2)} = \sum_i c_{i\alpha} c_{i\beta} f_i^{eq}. \tag{14}$$

Discrete Velocity Boltzmann Equation,

$$\frac{\partial f_i}{\partial t} + c_{i\alpha} \frac{\partial f_i}{\partial x_\alpha} = \Omega_i . \tag{15}$$

Mass and momentum conservations are obtained using moments, *e.g.* :

$$\frac{\partial \rho}{\partial t} + \frac{\partial \rho u_\alpha}{\partial x_\alpha} = \sum_i \Omega_i , \tag{16}$$

$$\frac{\partial \rho u_\alpha}{\partial t} + \frac{\partial \left[\rho u_\alpha u_\beta + p\delta_{\alpha\beta} + \Pi_{\alpha\beta}^{f^{neq},(2)}\right]}{\partial x_\beta} = \sum_i c_{i\alpha} \Omega_i , \tag{17}$$

Distributions or Moments ?

Lattice-Boltzmann with q velocities could be understood in 2 equivalent ways :

DVBE,

$$\frac{\partial f_i}{\partial t} + c_{i\alpha}\frac{\partial f_i}{\partial x_\alpha} = \Omega_i$$

describes q equations for f_i.

$\Leftrightarrow$

Extended hydrodynamic system,

$$\frac{\partial \Pi^{f,(n)}_{\alpha_1\cdots\alpha_n}}{\partial t} + \frac{\partial \Pi^{f,(n+1)}_{\alpha_1\cdots\alpha_n\alpha_{n+1}}}{\partial x_{\alpha_{n+1}}} = \Pi^{\Omega,(n)}_{\alpha_1\cdots\alpha_n}$$

describes q equations for $\Pi^{f,(n)}_{\alpha_1\cdots\alpha_n}$.

- What about boundary and initial conditions ?
- Which lattice closure, f^{eq} and collision kernel should be used ?
- What is the range of validity in term of Pr, Ma, Re, etc ?

"Higher-order hydrodynamics" is a research field by itself. Some of these models fail to reproduce physical results (*e.g.* Burnett with Bobylev instabilities).

➔ Can we avoid those uncertainties ? ➔

Lattice-Boltzmann is something in between **Boltzmann** and **Navier-Stokes-Fourier**.

➔ How to model compressible flows with Lattice-Boltzmann ? ⬅

Nowadays, Lattice-Boltzmann is a fully fledged numerical method used for different applications : fluids, solids, Schrödinger equation, finance, advection-diffusion etc...

➔ We can use classical tools : Taylor expansion and dimensional analysis. ⬅

Athermal Lattice-Boltzmann

Description of classical Lattice-Boltzmann

Athermal Lattice-Boltzmann-BGK

This model is summarized by

- **Equilibrium**,

$$f_i^{eq} = \omega_i \left\{ \mathcal{H}^{(0)}\rho + \frac{\mathcal{H}_{i\alpha}^{(1)}}{c_s^2}\rho u_\alpha + \frac{\mathcal{H}_{i\alpha\beta}^{(2)}}{2c_s^4}[\rho u_\alpha u_\beta] + \frac{\mathcal{H}_{i\alpha\beta\gamma}^{(3)}}{6c_s^6}[\rho u_\alpha u_\beta u_\gamma] \right\}. \quad (18)$$

- **Collide & stream**, BGK,

$$\overline{f}_i(t+\Delta t, \boldsymbol{x}) = \left\{ f_i^{eq} + \left(1 - \frac{\Delta t}{\tau + \Delta t/2}\right)\left[\overline{f}_i - f_i^{eq}\right] \right\}(t, \boldsymbol{x} - \boldsymbol{c}_i \Delta t). \quad (19)$$

- **Macroscopic reconstruction**,

$$\rho(t+\Delta t, \boldsymbol{x}) = \sum_{i=0}^{q-1} \overline{f}_i(t+\Delta t, \boldsymbol{x}), \quad (20)$$

$$\rho u_\alpha(t+\Delta t, \boldsymbol{x}) = \sum_{i=1}^{q-1} c_{i\alpha}\overline{f}_i(t+\Delta t, \boldsymbol{x}). \quad (21)$$

Where to find the stress-tensor ?

$$\frac{\partial \Pi^{f,(n)}_{\alpha_1\cdots\alpha_n}}{\partial t} + \frac{\partial \Pi^{f,(n+1)}_{\alpha_1\cdots\alpha_n\alpha_{n+1}}}{\partial x_{\alpha_{n+1}}} = -\frac{1}{\tau}\Pi^{f^{neq},(n)}_{\alpha_1\cdots\alpha_n} + \mathcal{O}(\Delta t^2) \qquad (22)$$

$$\downarrow \qquad \downarrow \qquad \downarrow \qquad \downarrow$$

n = 0 $$\frac{\partial \rho}{\partial t} + \frac{\partial \rho u_\beta}{\partial x_\beta} = \mathcal{O}(\Delta t^2)$$

n = 1 $$\frac{\partial \rho u_\alpha}{\partial t} + \frac{\partial \left[\rho u_\alpha u_\beta + \rho c_s^2 \delta_{\alpha\beta} + \Pi^{f^{neq},(2)}_{\alpha\beta}\right]}{\partial x_\beta} = \mathcal{O}(\Delta t^2)$$

n = 2 $$\frac{\partial \left[\Pi^{f^{eq},(2)}_{\alpha\beta} + \Pi^{f^{neq},(2)}_{\alpha\beta}\right]}{\partial t} + \frac{\partial \left[\Pi^{f^{eq},(3)}_{\alpha\beta\gamma} + \Pi^{f^{neq},(3)}_{\alpha\beta\gamma}\right]}{\partial x_\gamma} = -\frac{1}{\tau}\Pi^{f^{neq},(2)}_{\alpha\beta} + \mathcal{O}(\Delta t^2)$$

n = ... $$\cdots$$

The stress-tensor evolution equation is

$$
\begin{aligned}
-\Pi_{\alpha\beta}^{f^{neq},(2)} &= \tau\rho c_s^2\left[\frac{\partial u_\alpha}{\partial x_\beta}+\frac{\partial u_\beta}{\partial x_\alpha}\right]+\mathcal{O}\left(\tau\frac{\partial\rho u^3}{\partial x}\right)+\mathcal{O}(\Delta t^2)\\
&+\tau\frac{\partial\Pi_{\alpha\beta}^{f^{neq},(2)}}{\partial t}+\tau\frac{\partial\Pi_{\alpha\beta\gamma}^{f^{neq},(3)}}{\partial x_\gamma}-\tau\left[u_\alpha\frac{\partial\Pi_{\beta\gamma}^{f^{neq},(2)}}{\partial x_\gamma}+u_\beta\frac{\partial\Pi_{\alpha\gamma}^{f^{neq},(2)}}{\partial x_\gamma}\right]. \qquad (23)
\end{aligned}
$$

Usual low-Mach stress-tensor,

$$-\Pi_{\alpha\beta}^{f^{neq},(2)} \approx \underbrace{\tau\rho c_s^2}_{\mu}\left[\frac{\partial u_\alpha}{\partial x_\beta}+\frac{\partial u_\beta}{\partial x_\alpha}\right]. \qquad (24)$$

$\mathcal{O}\left(u^3\right)$ error,

$$\mathcal{O}\left(\tau\frac{\partial\rho u^3}{\partial x}\right)\propto u^3. \qquad (25)$$

Open system because $\Pi_{\alpha\beta\gamma}^{f^{neq},(3)}$ is unknown.

Time evolution.

The stress-tensor evolution equation is

$$-\Pi_{\alpha\beta}^{f^{neq},(2)} = \tau\rho c_s^2 \left[\frac{\partial u_\alpha}{\partial x_\beta} + \frac{\partial u_\beta}{\partial x_\alpha}\right] + \mathcal{O}\left(\tau\frac{\partial \rho u^3}{\partial x}\right) + \mathcal{O}(\Delta t^2)$$
$$+\tau\frac{\partial \Pi_{\alpha\beta}^{f^{neq},(2)}}{\partial t} + \tau\frac{\partial \Pi_{\alpha\beta\gamma}^{f^{neq},(3)}}{\partial x_\gamma} - \tau\left[u_\alpha\frac{\partial \Pi_{\beta\gamma}^{f^{neq},(2)}}{\partial x_\gamma} + u_\beta\frac{\partial \Pi_{\alpha\gamma}^{f^{neq},(2)}}{\partial x_\gamma}\right]. \quad (23)$$

Usual low-Mach stress-tensor,

$$-\Pi_{\alpha\beta}^{f^{neq},(2)} \approx \underbrace{\tau\rho c_s^2}_{\mu}\left[\frac{\partial u_\alpha}{\partial x_\beta} + \frac{\partial u_\beta}{\partial x_\alpha}\right]. \quad (24)$$

$\mathcal{O}\left(u^3\right)$ error,

$$\mathcal{O}\left(\tau\frac{\partial \rho u^3}{\partial x}\right) \propto u^3. \quad (25)$$

Open system because $\Pi_{\alpha\beta\gamma}^{f^{neq},(3)}$ is unknown.

Time evolution.

Athermal model : Constitutive equation

The stress-tensor evolution equation is

$$-\Pi^{f^{neq},(2)}_{\alpha\beta} = \tau\rho c_s^2 \left[\frac{\partial u_\alpha}{\partial x_\beta} + \frac{\partial u_\beta}{\partial x_\alpha}\right] + \mathcal{O}\left(\tau\frac{\partial \rho u^3}{\partial x}\right) + \mathcal{O}(\Delta t^2)$$
$$+\tau\frac{\partial \Pi^{f^{neq},(2)}_{\alpha\beta}}{\partial t} + \tau\frac{\partial \Pi^{f^{neq},(3)}_{\alpha\beta\gamma}}{\partial x_\gamma} - \tau\left[u_\alpha \frac{\partial \Pi^{f^{neq},(2)}_{\beta\gamma}}{\partial x_\gamma} + u_\beta \frac{\partial \Pi^{f^{neq},(2)}_{\alpha\gamma}}{\partial x_\gamma}\right]. \quad (23)$$

Usual low-Mach stress-tensor,

$$-\Pi^{f^{neq},(2)}_{\alpha\beta} \approx \underbrace{\tau\rho c_s^2}_{\mu} \left[\frac{\partial u_\alpha}{\partial x_\beta} + \frac{\partial u_\beta}{\partial x_\alpha}\right]. \quad (24)$$

$\mathcal{O}\left(u^3\right)$ error,

$$\mathcal{O}\left(\tau\frac{\partial \rho u^3}{\partial x}\right) \propto u^3. \quad (25)$$

Open system because $\Pi^{f^{neq},(3)}_{\alpha\beta\gamma}$ is unknown.

Time evolution.

Athermal model : Constitutive equation

The stress-tensor evolution equation is

$$-\Pi_{\alpha\beta}^{f^{neq},(2)} = \tau\rho c_s^2\left[\frac{\partial u_\alpha}{\partial x_\beta} + \frac{\partial u_\beta}{\partial x_\alpha}\right] + \mathcal{O}\left(\tau\frac{\partial\rho u^3}{\partial x}\right) + \mathcal{O}(\Delta t^2)$$
$$+\tau\frac{\partial\Pi_{\alpha\beta}^{f^{neq},(2)}}{\partial t} + \tau\frac{\partial\Pi_{\alpha\beta\gamma}^{f^{neq},(3)}}{\partial x_\gamma} - \tau\left[u_\alpha\frac{\partial\Pi_{\beta\gamma}^{f^{neq},(2)}}{\partial x_\gamma} + u_\beta\frac{\partial\Pi_{\alpha\gamma}^{f^{neq},(2)}}{\partial x_\gamma}\right]. \quad (23)$$

Usual low-Mach stress-tensor,

$$-\Pi_{\alpha\beta}^{f^{neq},(2)} \approx \underbrace{\tau\rho c_s^2}_{\mu}\left[\frac{\partial u_\alpha}{\partial x_\beta} + \frac{\partial u_\beta}{\partial x_\alpha}\right]. \quad (24)$$

$\mathcal{O}\left(u^3\right)$ error,

$$\mathcal{O}\left(\tau\frac{\partial\rho u^3}{\partial x}\right) \propto u^3. \quad (25)$$

Open system because $\Pi_{\alpha\beta\gamma}^{f^{neq},(3)}$ is unknown.

Time evolution.

Athermal model : Constitutive equation

The stress-tensor evolution equation is

$$
\begin{aligned}
-\Pi_{\alpha\beta}^{f^{neq},(2)} &= \tau\rho c_s^2\left[\frac{\partial u_\alpha}{\partial x_\beta}+\frac{\partial u_\beta}{\partial x_\alpha}\right]+\mathcal{O}\left(\tau\frac{\partial\rho u^3}{\partial x}\right)+\mathcal{O}(\Delta t^2)\\
&+\tau\frac{\partial\Pi_{\alpha\beta}^{f^{neq},(2)}}{\partial t}+\tau\frac{\partial\Pi_{\alpha\beta\gamma}^{f^{neq},(3)}}{\partial x_\gamma}-\tau\left[u_\alpha\frac{\partial\Pi_{\beta\gamma}^{f^{neq},(2)}}{\partial x_\gamma}+u_\beta\frac{\partial\Pi_{\alpha\gamma}^{f^{neq},(2)}}{\partial x_\gamma}\right]. \qquad (23)
\end{aligned}
$$

Usual low-Mach stress-tensor,

$$-\Pi_{\alpha\beta}^{f^{neq},(2)}\approx\underbrace{\tau\rho c_s^2}_{\mu}\left[\frac{\partial u_\alpha}{\partial x_\beta}+\frac{\partial u_\beta}{\partial x_\alpha}\right]. \qquad (24)$$

$\mathcal{O}\left(u^3\right)$ error,

$$\mathcal{O}\left(\tau\frac{\partial\rho u^3}{\partial x}\right)\propto u^3. \qquad (25)$$

Open system because $\Pi_{\alpha\beta\gamma}^{f^{neq},(3)}$ is unknown.

Time evolution.

Athermal constitutive equation, dimensional analysis 1/2

Assuming t_s is the shortest characteristic time, nondimensional variables * are $\mathcal{O}(1)$,

$$\frac{\partial}{\partial t} = \frac{1}{t_s}\frac{\partial}{\partial t^*}\,, \qquad \frac{\partial}{\partial x} = \frac{1}{L_0}\frac{\partial}{\partial x^*}\,, \tag{26}$$

$$\Pi^{f^{neq},(2)}_{\alpha\beta} = \Pi_0 \Pi^{*,f^{neq},(2)}_{\alpha\beta}\,, \qquad \Pi^{f^{neq},(3)}_{\alpha\beta\gamma} = Q_0 \Pi^{*,f^{neq},(3)}_{\alpha\beta\gamma}\,, \tag{27}$$

$$u = U_0 u^*\,, \qquad \rho = \rho_0 \rho^*\,, \qquad T = T_0 T^*\,, \tag{28}$$

neglecting numerical errors, the nondimensional stress-tensor is expressed as

$$-\Pi^{*,f^{neq},(2)}_{\alpha\beta} = \frac{\mu U_0}{L_0 \Pi_0}\left[\frac{\partial u^*_\alpha}{\partial x^*_\beta} + \frac{\partial u^*_\beta}{\partial x^*_\alpha}\right] + \mathcal{O}\left(\frac{\mu U_0}{L_0\Pi_0}\mathrm{Ma}^2\right)$$
$$+\,\mathcal{O}\left(\frac{\mu U_0}{L_0\Pi_0}\frac{Q_0}{\rho_0 c_s^2 U_0}\right) + \mathcal{O}\left(\frac{\tau}{t_s}\right) + \mathcal{O}\left(\frac{\mathrm{Ma}^2}{\mathrm{Re}}\right). \tag{29}$$

When the classical low-Mach constitutive equation is verified, only the blue part remains, in which case $\frac{\mu U_0}{L_0 \Pi_0} = 1$.

- $-\Pi^{*,f^{neq},(2)}_{\alpha\beta} = \left[\frac{\partial u^*_\alpha}{\partial x^*_\beta} + \frac{\partial u^*_\beta}{\partial x^*_\alpha}\right]$ "hydrodynamic limit".
- $\mathrm{Ma}^2 \ll 1$ error coming from u^3 isotropy defect can be neglected.
- $\frac{Q_0}{\rho_0 c_s^2 U_0} \ll 1$ higher-order contributions from $\Pi^{f^{neq},(3)}_{\alpha\beta\gamma}$ can be neglected.
- $\frac{\tau}{t_s} \ll 1$ stress-tensor time derivative can be neglected.
- $\frac{\mathrm{Ma}^2}{\mathrm{Re}} \ll 1$ other terms can be neglected.

➔ $\mathrm{Kn} \propto \mathrm{Ma}/\mathrm{Re}$ is not the only parameter that controls the consistency. ➔

Time evolution of f_i^{neq}

To get more insight on the interpretation of the non-equilibrium evolution, let recall the DVBE,

$$\frac{\partial f_i}{\partial t} + c_{i\alpha}\frac{\partial f_i}{\partial x_\alpha} = -\frac{1}{\tau}\left\{f_i - f_i^{eq}\right\} + \mathcal{O}\left(\Delta t^2\right) . \quad (30)$$

Let also recall that $f_i = f_i^{eq} + f_i^{neq}$ such that the DVBE yields,

$$\frac{\partial f_i^{neq}}{\partial t} + c_{i\alpha}\frac{\partial f_i^{neq}}{\partial x_\alpha} = -\frac{1}{\tau}\left\{f_i^{neq} - \Lambda_i\right\} + \mathcal{O}\left(\Delta t^2\right) , \quad (31)$$

with $\Lambda_i = \left[-\tau\frac{\partial f_i^{eq}}{\partial t} - \tau c_{i\alpha}\frac{\partial f_i^{eq}}{\partial x_\alpha}\right]$. f_i^{neq} relaxes towards Λ_i with a characteristic time τ.

➔ f_i^{neq} has its own "equilibrium" : Λ_i. ➔

Time evolution of f_i^{neq}

To get more insight on the interpretation of the non-equilibrium evolution, let recall the DVBE,

$$\frac{\partial f_i}{\partial t} + c_{i\alpha}\frac{\partial f_i}{\partial x_\alpha} = -\frac{1}{\tau}\left\{f_i - f_i^{eq}\right\} + \mathcal{O}\left(\Delta t^2\right) . \tag{30}$$

Let also recall that $f_i = f_i^{eq} + f_i^{neq}$ such that the DVBE yields,

$$\frac{\partial f_i^{neq}}{\partial t} + c_{i\alpha}\frac{\partial f_i^{neq}}{\partial x_\alpha} = -\frac{1}{\tau}\left\{f_i^{neq} - \Lambda_i\right\} + \mathcal{O}\left(\Delta t^2\right) , \tag{31}$$

with $\Lambda_i = \left[-\tau\frac{\partial f_i^{eq}}{\partial t} - \tau c_{i\alpha}\frac{\partial f_i^{eq}}{\partial x_\alpha}\right]$. f_i^{neq} relaxes towards Λ_i with a characteristic time τ.

➔ f_i^{neq} has its own "equilibrium" : Λ_i. ➔

Time evolution of $\Pi^{f^{neq},(2)}_{\alpha\beta}$

Hence, stress-tensor follows the compact equation,

$$\frac{\partial \Pi^{f^{neq},(2)}_{\alpha\beta}}{\partial t} + \frac{\partial \Pi^{f^{neq},(3)}_{\alpha\beta\gamma}}{\partial x_\gamma} = -\frac{1}{\tau}\left\{ \Pi^{f^{neq},(2)}_{\alpha\beta} - \Pi^{\Lambda,(2)}_{\alpha\beta} \right\} + \mathcal{O}\left(\Delta t^2\right) \, . \qquad (32)$$

- Small lattices $\rightarrow$ "isotropy defects" *e.g.* $\Pi^{(3)} \propto c_s^2 \Pi^{(1)}$ (this explains the $\mathcal{O}(u^3)$ error in stress-tensor).
- Isotropy defect is even worse for higher order moments.

➔ Closure : regularization, higher order moments are filtered. ⬅

Collision,

$$f_i^{coll} = f_i^{eq} + (1 - \Delta t/\overline{\tau})\overline{f}_i^{neq}\,, \tag{33}$$

can be projected onto moments,

$$\Pi^{coll,(3)} = \Pi^{eq,(3)} + (1 - \Delta t/\overline{\tau})\overline{\Pi}^{neq,(3)}\,, \tag{34}$$

$\overline{\Pi}^{neq,(3)}$ is regularized (replaced) by $\tilde{\Pi}^{neq,(3)}$,

$$\Pi^{coll,(3)} = \Pi^{eq,(3)} + (1 - \Delta t/\overline{\tau})\tilde{\Pi}^{neq,(3)}\,. \tag{35}$$

Exemple : When Latt & Chopard regularization is applied to D3Q19, the rank $q = 19$ of the solver is reduced to $\tilde{q} = 10$.

➔ We are not anymore solving the Discrete Velocity Boltzmann Equation ➔

Latt, J., & Chopard, B. *Lattice Boltzmann method with regularized pre-collision distribution functions.* Mathematics and Computers in Simulation. 2006

Collision,

$$f_i^{coll} = f_i^{eq} + (1 - \Delta t/\overline{\tau})\overline{f}_i^{neq} , \tag{33}$$

can be projected onto moments,

$$\Pi^{coll,(3)} = \Pi^{eq,(3)} + (1 - \Delta t/\overline{\tau})\overline{\Pi}^{neq,(3)} , \tag{34}$$

$\overline{\Pi}^{neq,(3)}$ is regularized (replaced) by $\tilde{\Pi}^{neq,(3)}$,

$$\Pi^{coll,(3)} = \Pi^{eq,(3)} + (1 - \Delta t/\overline{\tau})\tilde{\Pi}^{neq,(3)} . \tag{35}$$

Exemple : When Latt & Chopard regularization is applied to D3Q19, the rank $q = 19$ of the solver is reduced to $\tilde{q} = 10$.

➔ We are not anymore solving the Discrete Velocity Boltzmann Equation ➔

Latt, J., & Chopard, B. *Lattice Boltzmann method with regularized pre-collision distribution functions*, Mathematics and Computers in Simulation, 2006.

Regularized Lattice-Boltzmann model is obtained using Taylor expansion,

$$\frac{\partial \rho}{\partial t} + \frac{\partial \rho u_\beta}{\partial x_\beta} = \mathcal{O}(\Delta t^2), \tag{36}$$

$$\frac{\partial \rho u_\alpha}{\partial t} + \frac{\partial \left[\rho u_\alpha u_\beta + \rho c_s^2 \delta_{\alpha\beta} + \Pi^{f^{neq},(2)}_{\alpha\beta} \right]}{\partial x_\beta} = \mathcal{O}(\Delta t^2), \tag{37}$$

$$\frac{\partial \Pi^{f^{neq},(2)}_{\alpha\beta}}{\partial t} + \frac{\partial \tilde{\Pi}^{f^{neq},(3)}_{\alpha\beta\gamma}}{\partial x_\gamma} = -\frac{1}{\tau} \left\{ \Pi^{f^{neq},(2)}_{\alpha\beta} - \Pi^{\Lambda,(2)}_{\alpha\beta} \right\} + \mathcal{O}\left(\Delta t\right). \tag{38}$$

Stress-tensor evolution is $\mathcal{O}\left(\Delta t\right)$ accurate, but $\tilde{\Pi}^{neq,(3)}$ can be freely changed to increase stability/accuracy.

Thermal Lattice-Boltzmann

Hybrid coupling, entropy equation and traceless collision

Different paths towards thermal flows

Due to isotropy errors ($\Pi^{(3)} \propto c_s^2 \Pi^{(1)}$), energy conservation is wrong with standard lattices (*e.g.* D3Q19). Possible solutions,

- **Multispeed**, one large set of distributions. Computational efficiency is at stake. ✗

- **Double Distributions coupling**, 2 sets of distributions, one for mass/momentum and another for energy. Computational efficiency is at stake. ✗

- **Hybrid coupling**, 1 small set of distributions and 1 energy equation discretized by a finite difference scheme. Cheaper, allows coupling with a wide variety of models. ✓

The entropy equation in non-conservative form

The entropy is a mode of the linearized Euler system, its coupling with mass/momentum is weaker than using *e.g.* total energy or enthaply.

Entropy equation in the frame reference of a plane discontinuity,

$$u\frac{\partial s}{\partial x} = 0\,. \qquad (39)$$

Contact discontinuity is compatible. Shock is not, because $u \neq 0$ such that $\partial s/\partial x = 0$ is necessary.

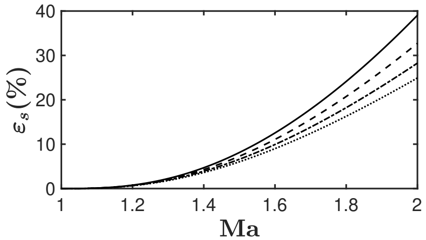

Figure 5: Entropy jump error with entropy equation as a function of Ma. $\gamma = 1.2, 1.4, 1.6, 1.8$ (top to bottom).

➔ Acceptable errors on plane shocks ($\sim 5\%$) up to Mach 1.4 ➔

Step-by-step Lattice-Boltzmann scheme from t to $t + \Delta t$

- **Initial solution**, $\rho(t, \boldsymbol{x})$, $u_\alpha(t, \boldsymbol{x})$, $T(t, \boldsymbol{x})$ and $\Pi_{\alpha\beta}^{f^{neq},(2)}(t, \boldsymbol{x})$ are known.

$\downarrow$ $\downarrow$

Lattice-Boltzmann

- Compute **Equilibrium** $f_i^{eq}(t, \boldsymbol{x})$ and **Non-Equilibrium** $\overline{f}_i^{neq}(t, \boldsymbol{x})$.
- **Collide & Stream** provides the updated distribution $\overline{f}_i(t + \Delta t, \boldsymbol{x})$.
- **Macroscopic update** provides $\rho(t + \Delta t, \boldsymbol{x})$ and $u_\alpha(t + \Delta t, \boldsymbol{x})$.

Finite Differences

- Compute the updated **Entropy** $s(t + \Delta t, \boldsymbol{x})$ using a one step explicit scheme. MUSCL-Hancock for advection and centered schemes for heat diffusion and viscous heat.

$\downarrow$ $\downarrow$

- **Temperature** update $T(t + \Delta t, \boldsymbol{x})$ using $\rho(t + \Delta t, \boldsymbol{x})$ and $s(t + \Delta t, \boldsymbol{x})$.
- **Stress-tensor** update $\Pi_{\alpha\beta}^{\overline{f}^{neq}}(t + \Delta t, \boldsymbol{x})$ using $\left[\Pi_{\alpha\beta}^{\overline{f}}, \rho, u_\alpha, T\right](t + \Delta t, \boldsymbol{x})$.

➔ Interface bewteen LBM/FD is the second order moment ➔

Step-by-step Lattice-Boltzmann scheme from t to $t + \Delta t$

- **Initial solution**, $\rho(t, \boldsymbol{x})$, $u_\alpha(t, \boldsymbol{x})$, $T(t, \boldsymbol{x})$ and $\Pi_{\alpha\beta}^{f^{neq},(2)}(t, \boldsymbol{x})$ are known.

$\downarrow$ $\downarrow$

Lattice-Boltzmann

- Compute **Equilibrium** $f_i^{eq}(t, \boldsymbol{x})$ and **Non-Equilibrium** $\overline{f}_i^{neq}(t, \boldsymbol{x})$.
- **Collide & Stream** provides the updated distribution $\overline{f}_i(t + \Delta t, \boldsymbol{x})$.
- **Macroscopic update** provides $\rho(t + \Delta t, \boldsymbol{x})$ and $u_\alpha(t + \Delta t, \boldsymbol{x})$.

Finite Differences

- Compute the updated **Entropy** $s(t + \Delta t, \boldsymbol{x})$ using a one step explicit scheme. MUSCL-Hancock for advection and centered schemes for heat diffusion and viscous heat.

$\downarrow$ $\downarrow$

- **Temperature** update $T(t + \Delta t, \boldsymbol{x})$ using $\rho(t + \Delta t, \boldsymbol{x})$ and $s(t + \Delta t, \boldsymbol{x})$.
- **Stress-tensor** update $\Pi_{\alpha\beta}^{\overline{f}^{neq}}(t + \Delta t, \boldsymbol{x})$ using $\left[\Pi_{\alpha\beta}^{\overline{f}}, \rho, u_\alpha, T\right](t + \Delta t, \boldsymbol{x})$.

➔ Interface bewteen LBM/FD is the second order moment ➔

Step-by-step Lattice-Boltzmann scheme from t to $t + \Delta t$

- **Initial solution**, $\rho(t, \boldsymbol{x})$, $u_\alpha(t, \boldsymbol{x})$, $T(t, \boldsymbol{x})$ and $\Pi^{f^{neq},(2)}_{\alpha\beta}(t, \boldsymbol{x})$ are known.

$\downarrow$ $\downarrow$

Lattice-Boltzmann

- Compute **Equilibrium** $f_i^{eq}(t, \boldsymbol{x})$ and **Non-Equilibrium** $\overline{f}_i^{neq}(t, \boldsymbol{x})$.
- **Collide & Stream** provides the updated distribution $\overline{f}_i(t + \Delta t, \boldsymbol{x})$.
- **Macroscopic update** provides $\rho(t + \Delta t, \boldsymbol{x})$ and $u_\alpha(t + \Delta t, \boldsymbol{x})$.

Finite Differences

- Compute the updated **Entropy** $s(t + \Delta t, \boldsymbol{x})$ using a one step explicit scheme. MUSCL-Hancock for advection and centered schemes for heat diffusion and viscous heat.

$\downarrow$ $\downarrow$

- **Temperature** update $T(t + \Delta t, \boldsymbol{x})$ using $\rho(t + \Delta t, \boldsymbol{x})$ and $s(t + \Delta t, \boldsymbol{x})$.
- **Stress-tensor** update $\Pi^{\overline{f}^{neq}}_{\alpha\beta}(t + \Delta t, \boldsymbol{x})$ using $\left[\Pi^{\overline{f}}_{\alpha\beta}, \rho, u_\alpha, T\right](t + \Delta t, \boldsymbol{x})$.

➔ Interface bewteen LBM/FD is the second order moment ➔

Step-by-step Lattice-Boltzmann scheme from t to $t+\Delta t$

- **Initial solution**, $\rho(t,\boldsymbol{x})$, $u_\alpha(t,\boldsymbol{x})$, $T(t,\boldsymbol{x})$ and $\Pi_{\alpha\beta}^{f^{neq},(2)}(t,\boldsymbol{x})$ are known.

$\downarrow$ $\downarrow$

Lattice-Boltzmann

- Compute **Equilibrium** $f_i^{eq}(t,\boldsymbol{x})$ and **Non-Equilibrium** $\overline{f}_i^{neq}(t,\boldsymbol{x})$.
- **Collide & Stream** provides the updated distribution $\overline{f}_i(t+\Delta t,\boldsymbol{x})$.
- **Macroscopic update** provides $\rho(t+\Delta t,\boldsymbol{x})$ and $u_\alpha(t+\Delta t,\boldsymbol{x})$.

Finite Differences

- Compute the updated **Entropy** $s(t+\Delta t,\boldsymbol{x})$ using a one step explicit scheme. MUSCL-Hancock for advection and centered schemes for heat diffusion and viscous heat.

$\downarrow$ $\downarrow$

- **Temperature** update $T(t+\Delta t,\boldsymbol{x})$ using $\rho(t+\Delta t,\boldsymbol{x})$ and $s(t+\Delta t,\boldsymbol{x})$.
- **Stress-tensor** update $\Pi_{\alpha\beta}^{\overline{f}^{neq}}(t+\Delta t,\boldsymbol{x})$ using $\left[\Pi_{\alpha\beta}^{\overline{f}},\rho,u_\alpha,T\right](t+\Delta t,\boldsymbol{x})$.

➔ Interface bewteen LBM/FD is the second order moment 🡸

$\Pi^{\overline{f}^{neq}}_{\alpha\beta}$ uses $\Pi^{\overline{f}}_{\alpha\beta}$, ρ, u_α (LBM) and p (LBM/FD),

$$\begin{aligned}\Pi^{\overline{f}^{neq}}_{\alpha\beta} &= \left(\Pi^{\overline{f}}_{\alpha\beta} - \Pi^{f^{eq}}_{\alpha\beta}\right) \\ &= \left(\Pi^{\overline{f}}_{\alpha\beta} - \left[\rho u_\alpha u_\beta + p\delta_{\alpha\beta}\right]\right) .\end{aligned} \tag{40}$$

Coupling errors between LBM/FD are stacked in the trace of $\Pi^{\overline{f}^{neq}}_{\alpha\beta}$.

A compressible scheme traditionally uses Stokes Hypothesis (traceless $\Pi^{f^{neq},(2)}_{\alpha\beta}$),

$$-\Pi^{f^{neq},(2)}_{\alpha\beta} = \mu\left[\frac{\partial u_\alpha}{\partial x_\beta} + \frac{\partial u_\beta}{\partial x_\alpha} - \frac{2\delta_{\alpha\beta}}{3}\frac{\partial u_\gamma}{\partial x_\gamma}\right] , \tag{41}$$

The trace $\Pi^{\overline{f}^{neq}}_{\alpha\alpha}$ is pure errors, it could be safely replaced by 0.

➔ New regularization $\Pi^{\overline{f}^{neq}}_{\alpha\alpha} = 0$ improves the stability. ➔

Farag, G. & Zhao, S. & Coratger, T. & Boivin, P. & Sagaut, P. A pressure-based regularized lattice-Boltzmann method for the simulation of compressible flows, Physics of Fluids, 2020.

Thermal coupling, traceless collision

$\Pi^{\overline{f}^{neq}}_{\alpha\beta}$ uses $\Pi^{\overline{f}}_{\alpha\beta}$, ρ, u_α (LBM) and p (LBM/FD),

$$\begin{aligned}\Pi^{\overline{f}^{neq}}_{\alpha\beta} &= \left(\Pi^{\overline{f}}_{\alpha\beta} - \Pi^{f^{eq}}_{\alpha\beta}\right) \\ &= \left(\Pi^{\overline{f}}_{\alpha\beta} - \left[\rho u_\alpha u_\beta + p\delta_{\alpha\beta}\right]\right) .\end{aligned} \tag{40}$$

Coupling errors between LBM/FD are stacked in the trace of $\Pi^{\overline{f}^{neq}}_{\alpha\beta}$.

A compressible scheme traditionally uses Stokes Hypothesis (traceless $\Pi^{f^{neq},(2)}_{\alpha\beta}$),

$$-\Pi^{f^{neq},(2)}_{\alpha\beta} = \mu\left[\frac{\partial u_\alpha}{\partial x_\beta} + \frac{\partial u_\beta}{\partial x_\alpha} - \frac{2\delta_{\alpha\beta}}{3}\frac{\partial u_\gamma}{\partial x_\gamma}\right] , \tag{41}$$

The trace $\Pi^{\overline{f}^{neq}}_{\alpha\alpha}$ is pure errors, it could be safely replaced by 0.

➔ New regularization $\Pi^{\overline{f}^{neq}}_{\alpha\alpha} = 0$ improves the stability. ➔

Farag, G. & Zhao, S. & Coratger, T. & Boivin, P. & Sagaut, P. *A pressure-based regularized lattice-Boltzmann method for the simulation of compressible flows*, Physics of Fluids, 2020.

Compressible models & applications

Pressure-based model, unified model, applications

M2P2 Lattice-Boltzmann models 1/2

During the past few years, M2P2 designed different compressible models,

- Density based (ρ-based), 2019,
  - **Y. Feng, P. Boivin, J. Jacob and P. Sagaut**. Hybrid recursive regularized thermal lattice Boltzmann model for high subsonic compressible flows. Journal of Computational Physics, 2019.
  - **F. Renard, Y. Feng, , JF. Boussuge and P. Sagaut**. Improved compressible Hybrid Lattice Boltzmann Method on standard lattice for subsonic and supersonic flows. Computers & Fluids, 2021.
- Pressure based (p-based), early 2020,
  - **G. Farag, S. Zhao, T. Coratger, P. Boivin, G. Chiavassa and P. Sagaut**. A pressure-based regularized lattice-Boltzmann method for the simulation of compressible flows. Physics of Fluids, 2020.
- Improved-density based ($i\rho$-based), late 2020,
  - **S. Guo, Y. Feng and P. Sagaut**. Improved standard thermal lattice Boltzmann model with hybrid recursive regularization for compressible laminar and turbulent flows. Physics of Fluids, 2020.

➔ How do they differ from one another ? Which one should be used ? ➔

Their 2^{nd}-order distributions are :

$$f_i^{\rho,eq} = \omega_i \left\{ \rho + \frac{\mathcal{H}^{(1)}_{i\alpha}}{c_s^2} \rho u_\alpha + \frac{\mathcal{H}^{(2)}_{i\alpha\beta}}{2c_s^4} \left[\rho u_\alpha u_\beta + \delta_{\alpha\beta} \rho c_s^2 (\theta - 1) \right] \right\} \tag{42}$$

$$f_i^{p,eq} = \omega_i \left\{ \rho\theta + \frac{\mathcal{H}^{(1)}_{i\alpha}}{c_s^2} \rho u_\alpha + \frac{\mathcal{H}^{(2)}_{i\alpha\beta}}{2c_s^4} \left[\rho u_\alpha u_\beta + \delta_{\alpha\beta} 0 \right] \right\} \tag{43}$$

$$f_i^{i\rho,eq} = \omega_i \left\{ \rho + \frac{\mathcal{H}^{(1)}_{i\alpha}}{c_s^2} \rho u_\alpha + \frac{\mathcal{H}^{(2)}_{i\alpha\beta}}{2c_s^4} \left[\rho u_\alpha u_\beta + \delta_{\alpha\beta} 0 \right] + \frac{\omega_i - \delta_{0i}}{\omega_i} \rho [\theta - 1] \right\} \tag{44}$$

With 2 different update rules for mass :

- $\rho / i\rho$-based : $\rho(t + \Delta t, \boldsymbol{x}) = \sum_{i=0}^{q-1} \overline{f}_i(t + \Delta t, \boldsymbol{x})$ (45)
- p-based : $\rho(t + \Delta t, \boldsymbol{x}) = \sum_{i=0}^{q-1} \overline{f}_i(t + \Delta t, \boldsymbol{x}) + \rho(t, \boldsymbol{x})[1 - \theta(t, \boldsymbol{x})]$ (46)

➔ Very close equations, let us try to find a generalized formulation. ➔

A generalized equilibrium on D3Q19

Considering the D3Q19 lattice a function can be projected onto its basis

$$\Big(\mathcal{H}_i^{(0)}, \mathcal{H}_{ix}^{(1)}, \mathcal{H}_{iy}^{(1)}, \mathcal{H}_{iz}^{(1)}, \mathcal{H}_{ixx}^{(2)}, \mathcal{H}_{iyy}^{(2)}, \mathcal{H}_{izz}^{(2)}, \mathcal{H}_{ixy}^{(2)}, \mathcal{H}_{ixz}^{(2)}, \mathcal{H}_{iyz}^{(2)}, \mathcal{H}_{ixxy}^{(3)}, \mathcal{H}_{ixxz}^{(3)}, \mathcal{H}_{iyyx}^{(3)}, \mathcal{H}_{iyyz}^{(3)}, \mathcal{H}_{izzx}^{(3)}, \mathcal{H}_{izzy}^{(3)}, \mathcal{A}_i, \mathcal{B}_i, \mathcal{C}_i\Big) \tag{47}$$

The equilibrium distribution that generalizes M2P2 models is

$$f_i^{eq} = \omega_i \Big\{ \mathcal{H}^{(0)}\rho + \frac{\mathcal{H}_{i\alpha}^{(1)}}{c_s^2}\rho u_\alpha + \frac{\mathcal{H}_{i\alpha\beta}^{(2)}}{2c_s^4}\left[\rho u_\alpha u_\beta + \delta_{\alpha\beta}\rho c_s^2(\theta - 1)\right] + \frac{\mathcal{H}_{i\alpha\beta\gamma}^{(3)}}{6c_s^6}\Big[\rho u_\alpha u_\beta u_\gamma - \kappa\rho c_s^2\left(u_\alpha\delta_{\beta\gamma} + u_\beta\delta_{\gamma\alpha} + u_\gamma\delta_{\alpha\beta}\right)\Big] - \frac{\mathcal{A}_i + \mathcal{B}_i + \mathcal{C}_i}{12c_s^4}\rho[\theta - 1](1 - \zeta)\Big\}. \tag{48}$$

- $\zeta = 1$ and $\kappa = 1 - \theta$ is the classical ρ-based.
- $\zeta = 0$ and $\kappa = 0$ is for p-based and $i\rho$-based. Same core model !

➔ Differences between models are inside 3^{rd} and 4^{th}-order moments. ➔

Unified model on D3Q19, ingredients

1/ **Classical thermal equilibrium up to 2^{nd}-order** ➔ Consistent mass and momentum Euler conservation.

2/ **Higher-order equilibrium moments related to $\mathcal{A}_i$ $\mathcal{B}_i$ and $\mathcal{C}_i$ polynomials and force correction term similar to pressure-based model** ➔ Improved stability.

3/ **Athermal 3^{rd} order equilibrium moments $\rho u_\alpha u_\beta u_\gamma$** ➔ Improved stability and more reasonable errors $\mathcal{O}(\frac{\mathrm{Ma}^2\mathrm{CFL}^2}{\mathrm{Re}(\mathrm{Ma}+1)^2})$ compared to $\mathcal{O}(\frac{\mathrm{Ma}^2}{\mathrm{Re}}) + \mathcal{O}(\frac{1}{\mathrm{RePr}})$ in classical density-based thermal model.

4/ **Entropy equation using MUSCL-Hancock scheme** ➔ Reasonable trade-off between small stencil (1D is 5points), both stability and accuracy are improved.

5/ **Discontinuity sensor based on density** ➔ Increased viscosity in both shocks and contact discontinuities.

6/ **Small artificial bulk viscosity** ➔ Necessary for very high Mach $\gtrapprox 1.7$.

7/ **Recursive regularization and regularization of stress-tensor trace** ➔ Improved stability.

Farag, G. & Coratger, T. & Wissocq G. & Zhao S. & Boivin P. & Sagaut P. *A unified hybrid lattice-Boltzmann method for compressible flows: Bridging between pressure-based and density-based methods*, Physics of Fluids, 2021.

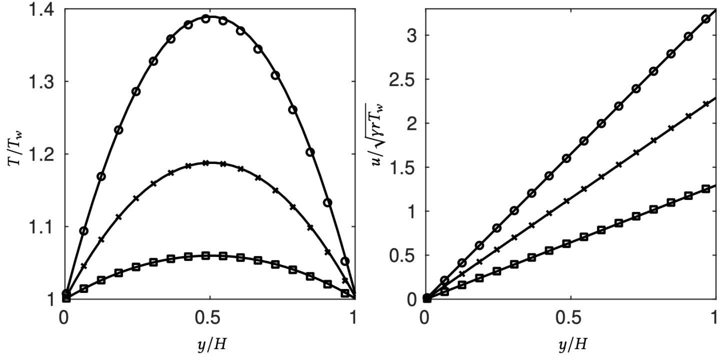

Figure 6: □, × and ◯ are the Ma = 1.3, 2.3, 3.3 analytical solution.
—— correspond to numerical solutions with the unified model.

100 × 1 × 1 mesh, CFL ranging between 0.5 and 0.2.

➔ Accurate viscosity, heat diffusion and viscous heat ➔

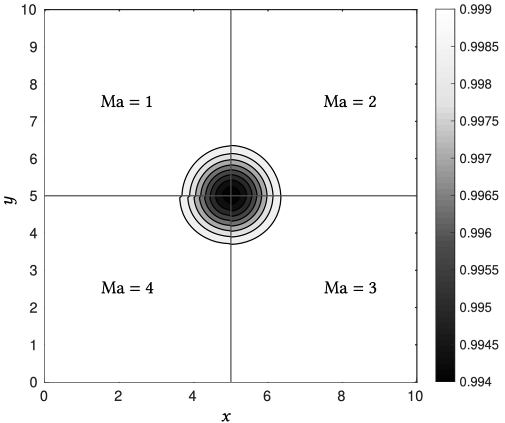

Figure 7: Isentropic vortex advection after 20 flow-through-time periods for different Mach numbers.

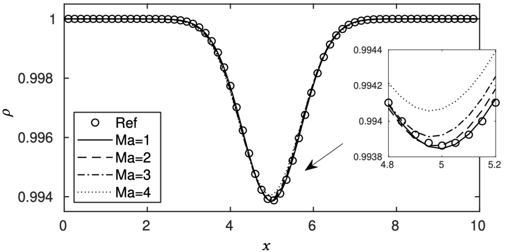

Figure 8: $y = 0$ density slices after 20 periods for different Ma.

$200 \times 200 \times 1$ mesh, CFL from 0.3 to 0.1 and $\mu = 0$.

➔ Low numerical dissipation/dispersion ➔

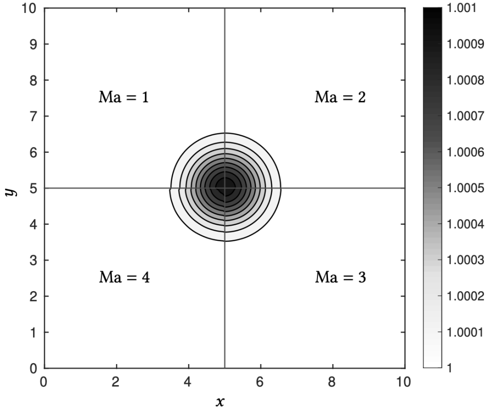

Figure 9: Entropy spot advection after 20 flow-through-time periods for different Mach numbers.

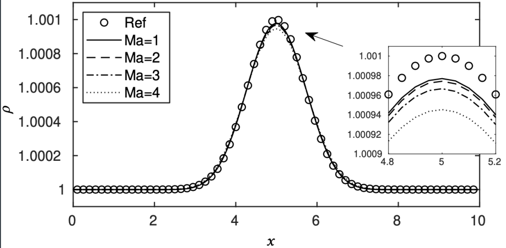

Figure 10: $y = 0$ density slices after 20 periods for different Ma.

$200 \times 200 \times 1$ mesh, CFL from 0.3 to 0.1 and $\mu = 0$.

➔ Low numerical dissipation/dispersion 🡐

Unified model : 2D Riemann problems

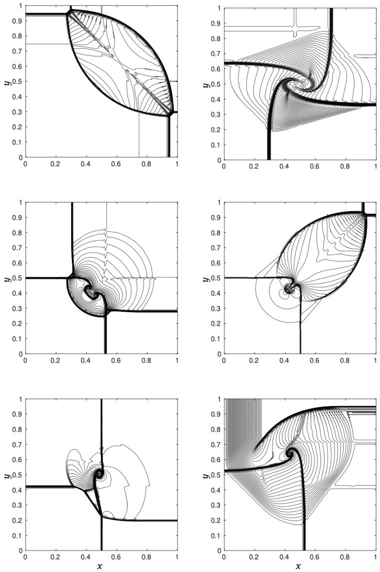

Figure 11: Lax & Liu 2D Riemann problems : Density fields of configurations 4-6-11-12-13-16.

$400 \times 400 \times 1$ grid, $\Delta t / \Delta x = 0.22$ extremely close to Lax & Liu's article, $\mu = 0$ and discontinuity sensor.

➔ Robust ⬅

Unified model : Compressible double shear layer

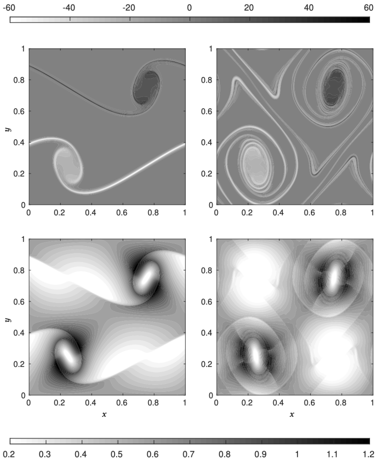

Figure 12: Vorticity (top) and Mach (bottom) at time t_c (left) and $2t_c$ (right) using the 512×512 grid.

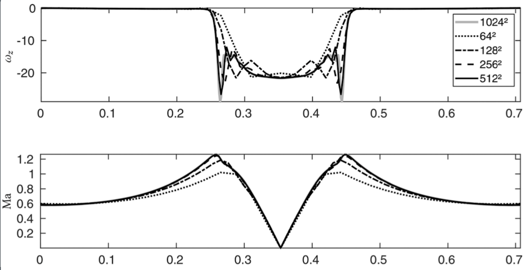

Figure 13: Diagonal Vorticity and Mach slices at time t_c for different resolutions.

Initial CFL $= 0.28$ and $\mu = 0$.

➔ Robust ➔

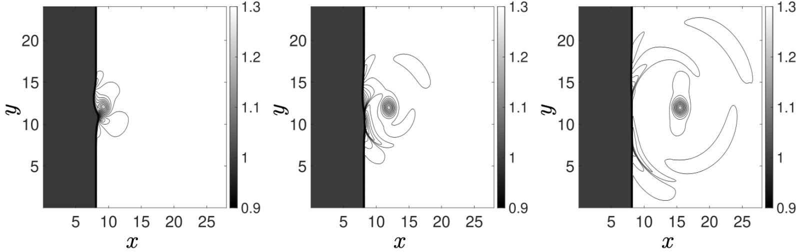

Figure 14: Vortex/shock interaction : density fields at time $t = 3, 6, 10$.

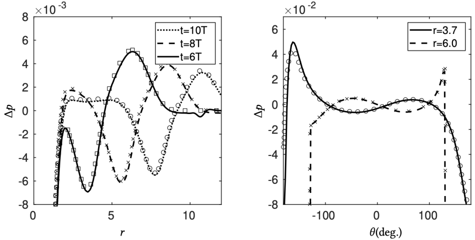

Figure 15: Different acoustic slices compared to reference.

CFL $= 0.83$ and discontinuity sensor.
Other parameters are identical to reference.
➔ Robust ⬅

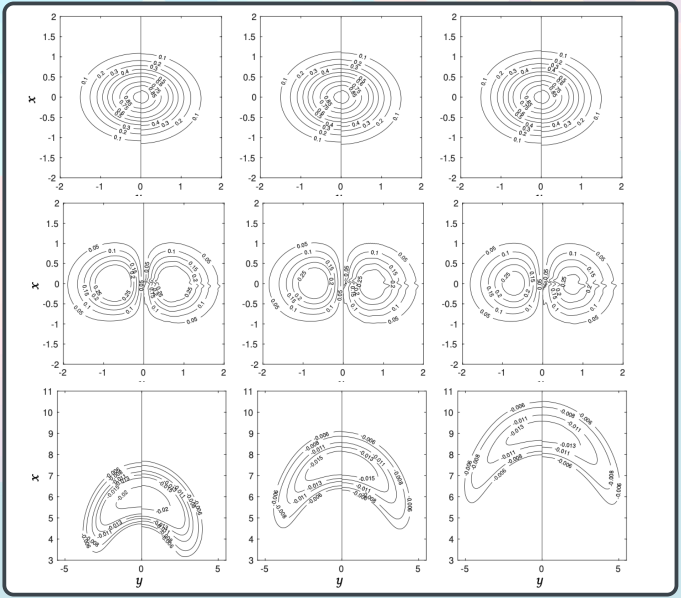

Figure 16: Transmitted entropy, vorticity and pressure fields. From left to right $\gamma = 1.2$, 1.4 and 1.6. Analytical and numerical solutions respectively correspond to $y < 0$ and $y \geq 0$.

Initial CFL $= 0.42$ and $\mu = 0$.

➔ Robust ⬅

Conclusion

1/ In the absence of a careful study of higher-order terms, the Lattice-Boltzmann link with kinetic theory is blurred.

2/ $\Delta t \to 0$ is the sole necessary assumption to study a LB model. Being cheaper in term of assumptions, the dimensional analysis outperforms Chapman-Enskog.

3/ M2P2 models are now unified under a single formalism.

4/ "Kinetic-theory-inspired" LB schemes is not necessarily the most efficient path towards stability/accuracy.

5/ The regularization has been extended to the trace of the stress-tensor : $\Pi^{neq}_{\alpha\alpha}$. This drastically improves the stability.

Short bibliography

J. Latt & B. Chopard. *Lattice Boltzmann method with regularized pre-collision distribution functions*, Mathematics and Computers in Simulation, 2006.

F. Dubois. *Equivalent partial differential equations of a lattice Boltzmann scheme*, Computers & Mathematics with Applications, 2008.

C. Coreixas, G. Wissocq, G. Puigt, J. F. Boussuge & P. Sagaut. *Recursive regularization step for high-order lattice Boltzmann methods*, Physical Review E, 2017.

J. Jacob, O. Malaspinas & P. Sagaut. *A new hybrid recursive regularised Bhatnagar–Gross–Krook collision model for Lattice Boltzmann method-based large eddy simulation*, Journal of Turbulence, 2018.

Y. Feng, P. Boivin, J. Jacob & P. Sagaut *Hybrid recursive regularized thermal lattice Boltzmann model for high subsonic compressible flows*, Journal of Computational Physics, 2019.

G. Farag, S. Zhao, T. Coratger, P. Boivin & P. Sagaut. *A pressure-based regularized lattice-Boltzmann method for the simulation of compressible flows*, Physics of Fluids, 2020.

S. Guo, Y. Feng & P. Sagaut *Improved standard thermal lattice Boltzmann model with hybrid recursive regularization for compressible laminar and turbulent flows*, Physics of Fluids, 2020.

G. Farag, S. Zhao, G. Chiavassa & P. Boivin. *Consistency study of Lattice-Boltzmann schemes macroscopic limit*, Physics of Fluids, 2021.

F. Renard, Y. Feng, , JF. Boussuge & P. Sagaut *Improved compressible Hybrid Lattice Boltzmann Method on standard lattice for subsonic and supersonic flows*, Computers & Fluids, 2021.

G. Farag, T. Coratger, G. Wissocq, S. Zhao, P. Boivin & P. Sagaut. *A unified hybrid lattice-Boltzmann method for compressible flows: Bridging between pressure-based and density-based methods*, Physics of Fluids, 2021.

G. Wissocq & P. Sagaut. *Hydrodynamic limits and numerical errors of isothermal lattice Boltzmann schemes*, Journal of Computational Physics, 2022.